MODELING OF CONCRETE MATERIALS AND STRUCTURES

Kaspar Willam, University of Colorado at Boulder
In cooperation with Bernd Köberl, Technical University of Vienna, Austria.

Class Meeting #6: Tension Softening vs Tension Stiffening

Smeared Crack Approach: *Plastic Softening (isotropic case)*

Axial Force Member in Tension and Compression: *Snap-Back Effect*

Cross-Effect: *Lateral Confinement due Mismatch in 3-D*

Tension Stiffening: *Debonding in Reinforced Concrete*

TENSION SOFTENING AND APPARENT DUCTILITY

Tensile Cracking:

Smeared Crack Approach vs Plastic Softening.

Axial Force Problem:

Serial Structure-Localization in Weakest Link.

Localization of Axial Deformation:

Snap-Back and 3-D Cross-Effect when elastic energy release exceeds dissipation in softening domain.

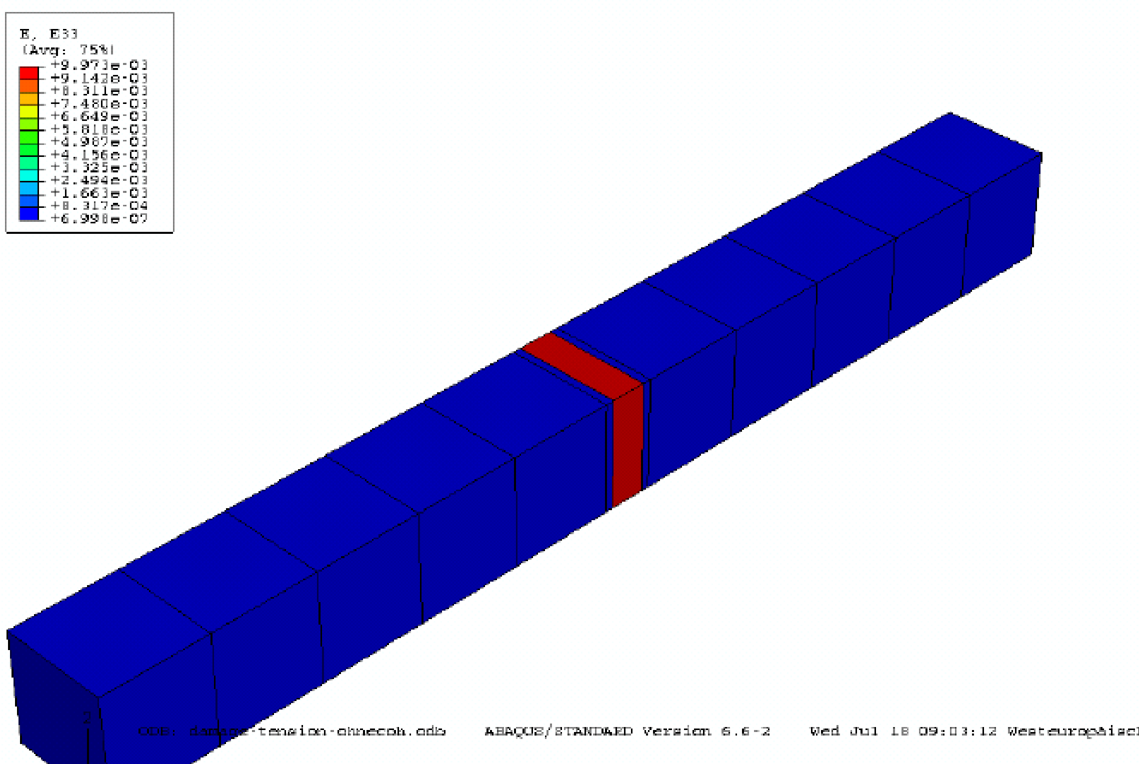

TENSION SOFTENING

Tensile Failure of Axial Force Member:

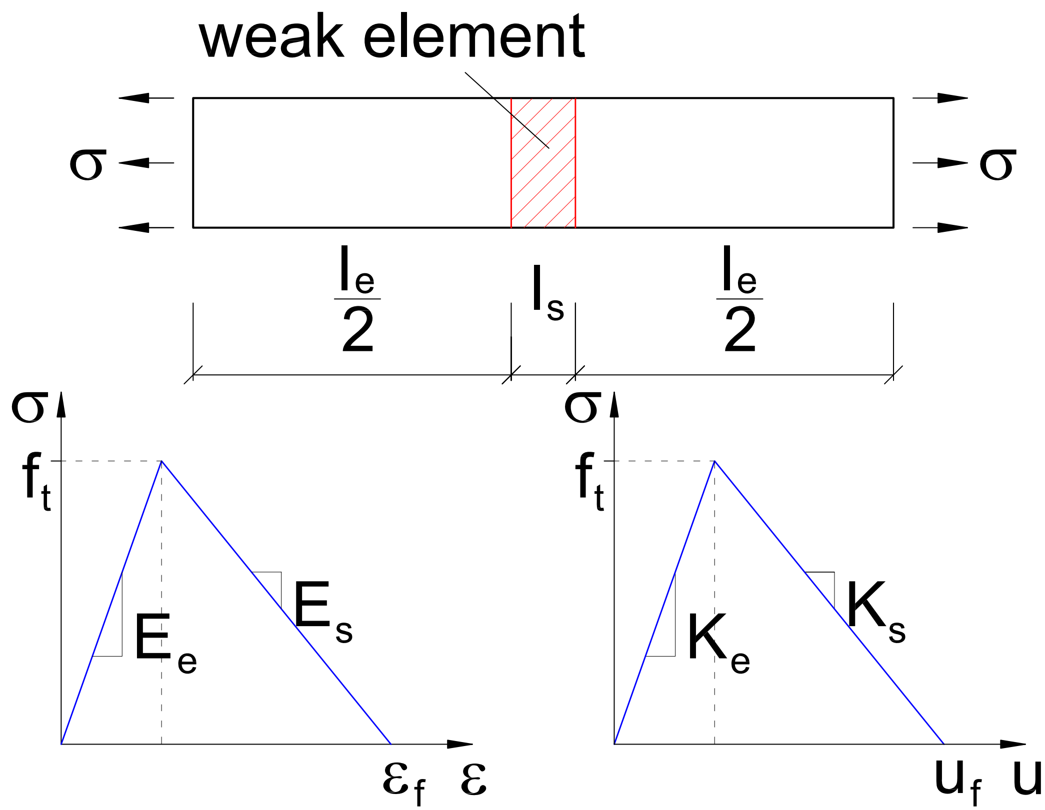

1-D PLASTIC HARDENING/SOFTENING

Elastic-Plastic Decomposition:

$$\dot{\epsilon} = \dot{\epsilon}_e + \dot{\epsilon}_p \quad \text{where} \quad \dot{\epsilon}_e = \frac{\dot{\sigma}}{E_e} \quad \text{and} \quad \dot{\epsilon}_p = \frac{\dot{\sigma}}{E_p}$$

Consequently,

$$\dot{\epsilon} = \frac{\dot{\sigma}}{E_e} + \frac{\dot{\sigma}}{E_p} = \frac{\dot{\sigma}}{E_{tan}}$$

Elastoplastic Tangent Stiffness Relationship:

$$\dot{\sigma} = E_{tan}\dot{\epsilon} \quad \text{where} \quad E_{tan} = \frac{E_e E_p}{E_e + E_p}$$

Note: $E_{tan} = -\infty$
when $E_p^{crit} = -E_e$.

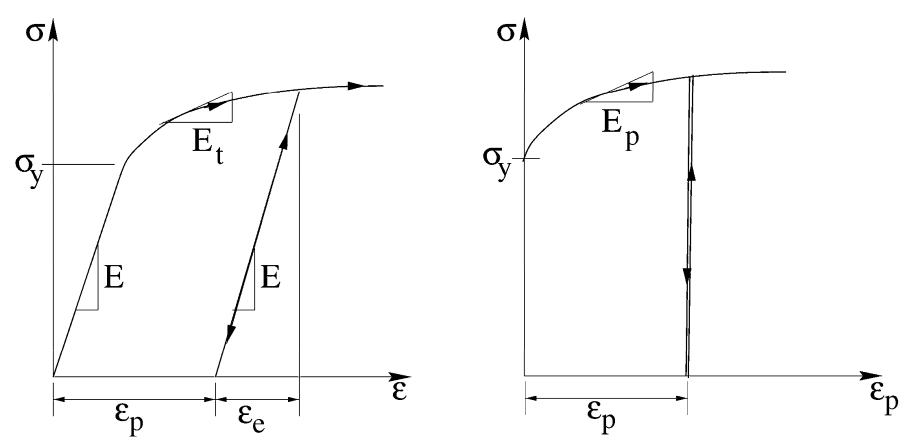

3-D PLASTIC SOFTENING

Rankine Criterion for Tension Cut-Off: $F_R(\boldsymbol{\sigma}, \kappa) = \sigma_1 - f_t(\kappa) = 0$

Associated Plastic Flow Rule: $\dot{\boldsymbol{\epsilon}}^p = \dot{\lambda}\boldsymbol{m}$ where $\dot{\epsilon}_1^p = \dot{\lambda}\, sign(\sigma_1)$

Isotropic Strain Softening Rule: $f_t(\kappa) = f_t + E_p\kappa$ where $-E < E_p < 0$.

Plastic Consistency: $\dot{F}_R(\boldsymbol{\sigma}, \kappa) = \dot{\sigma}_1 - E_p\dot{\kappa} = 0.$

Strain-driven Format: from $\dot{\kappa} = \dot{\epsilon}_1^p = \dot{\lambda}$ we find $\dot{\lambda} = \frac{E}{E+E_p}\dot{\epsilon}_1$

Tangent Stiffness Format: $\dot{\sigma}_1 = E[\dot{\epsilon}_1 - \dot{\lambda}] = E_{tan}\dot{\epsilon}_1$ where $E_{tan} = \frac{EE_p}{E+E_p}$

Fracture Energy Based Softening:

$$E_p = \frac{d\sigma_1}{d\epsilon_1^p} = \frac{d\sigma_1}{du_N^f}\frac{du_N^f}{d\epsilon_1^p} = K_p\, s$$

where $s = crack\ separation$

$$G_f^I = \int_u^f \sigma_1 du_N^f = \frac{1}{2} f_t\, u_{cr}^f$$

Critical Softening:

$$E_p^{crit} = K_p^{crit}\, s = -E_e$$

or $K_p^{crit} = -\frac{E_e}{s}$

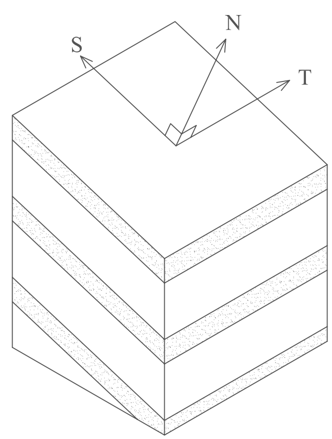

Smeared Cracking

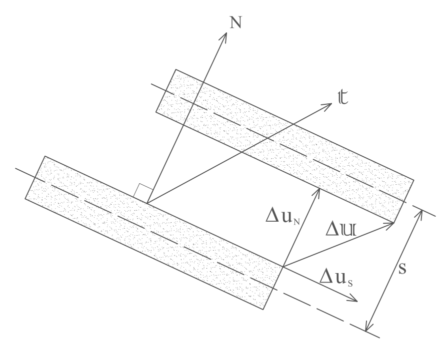

Traction - Separation t - Δu

WEAK ELEMENT IN AXIAL FORCE MEMBER

Snap-Back Analysis of Serial Structure:

Static Equilibrium: $\Delta\sigma_{axial} = \Delta\sigma_e = \Delta\sigma_s$

Total Change of Length of Axial Force Member: $\Delta\ell = \Delta\ell_e + \Delta\ell_s$

$$\Delta\ell = \frac{\Delta\sigma_e}{E_e}\ell_e + \frac{\Delta\sigma_s}{E_s}\ell_s$$

and

$$\Delta\sigma_{axial} = \frac{E_e E_s}{E_e\ell_s + E_s\ell_e}\Delta\ell$$

Controllable Softening Range as long as:

$$E_e\ell_s + E_s\ell_e > 0$$

TENSION SOFTENING

Critical Size of Softening Zone for Snap-Back:

$$\ell_s^{crit} = -\frac{E_s}{E_e}\ell_e$$

Note Snap-Back in spite of Constant Fracture Energy: $G_f = const$

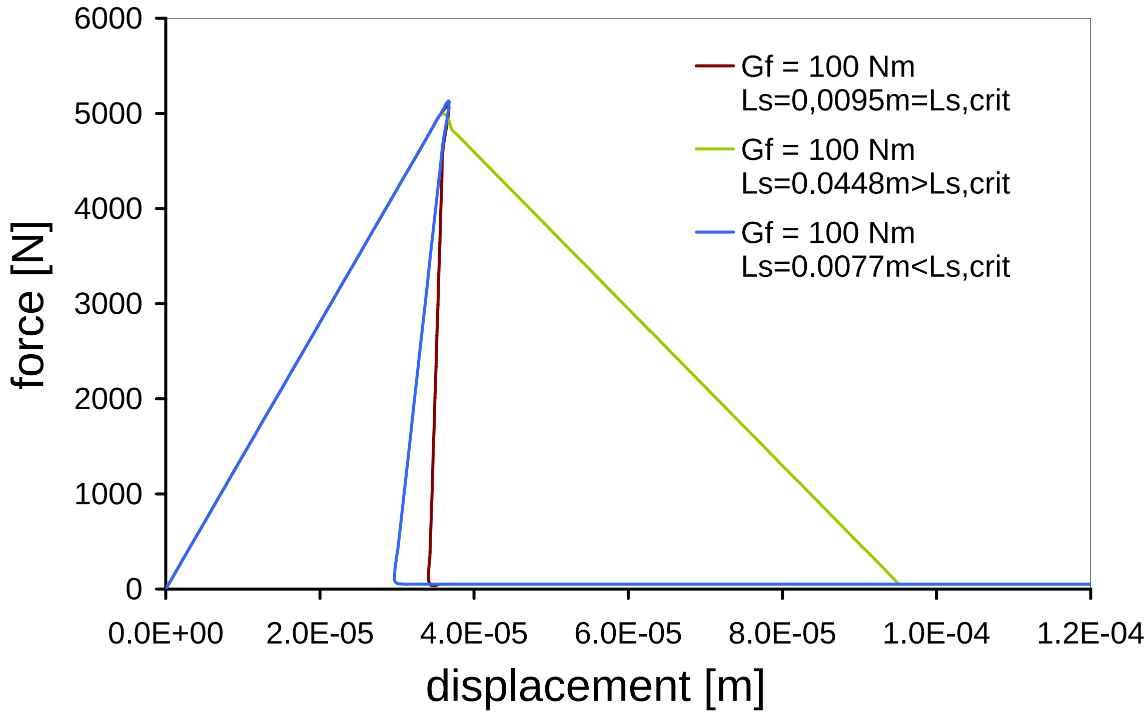

TENSION SOFTENING

Cohesive Interface Approach: Strong Discontinuity

$$\Delta\sigma = \frac{K_s E_e}{E_e + K_s \ell_e}\Delta\ell \quad \text{snap-back when} \quad {\ell_e}^{crit} = 2\frac{E_e G_f^{crit}}{f_t^2}$$

Note: ${\ell_e}^{crit}$ compares with characteristic length of Hillerborg et al.

Effect of different G_f values on Structural Softening:

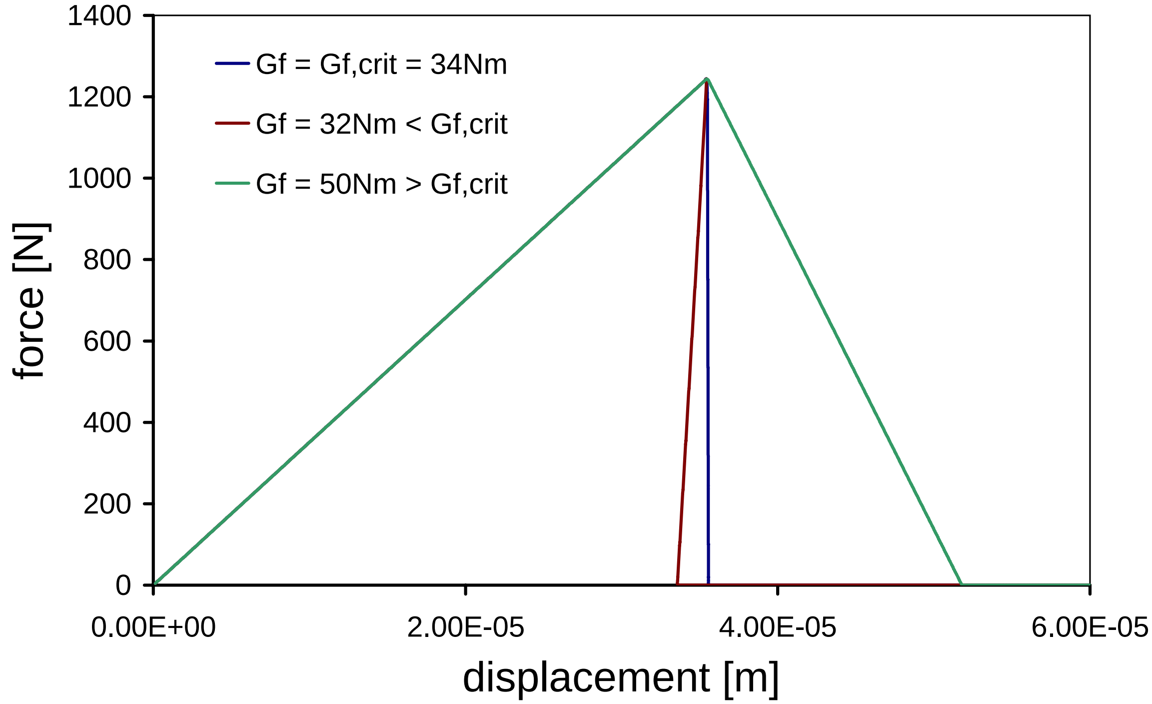

TENSION SOFTENING

Fracture energy-based softening: Linear vs Exponential Format

Mesh-size dependent softening modulus: $E_s = \frac{d\sigma}{du_f}\frac{du_f}{d\epsilon_f} = K_s h_{el}$

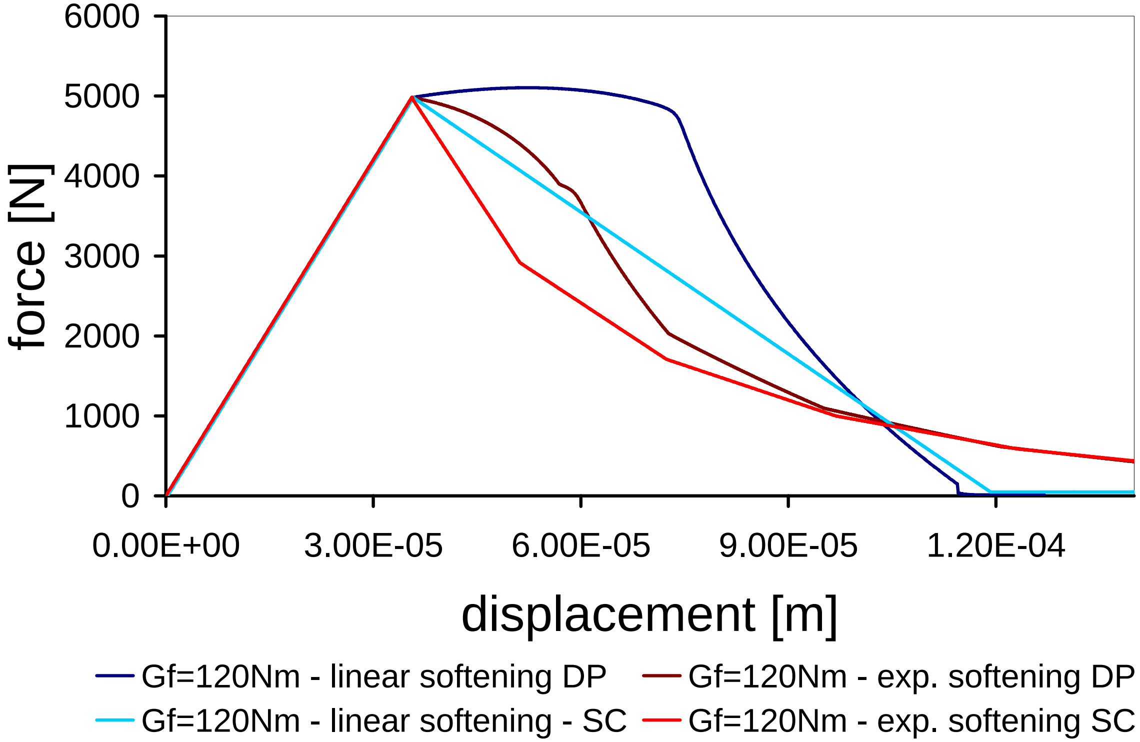

TENSION SOFTENING

3-D Cross Effects: of Damage-Plasticity Model in Abaqus

Displacement Continuity introduces lateral confinement

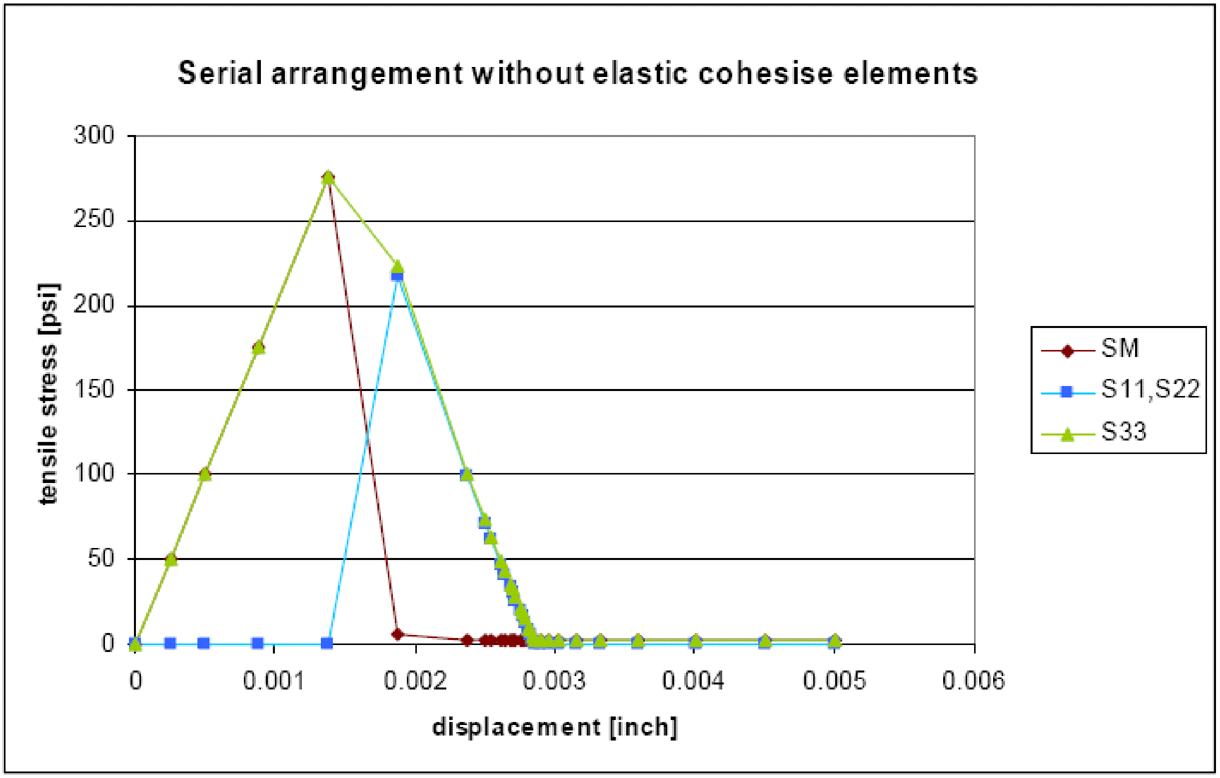

TENSION SOFTENING

3-D Cross Effects Eliminated by Shear Slip and Loss of Bond

Insert zero shear interface elements between weak softening element and elastic unloading elements.

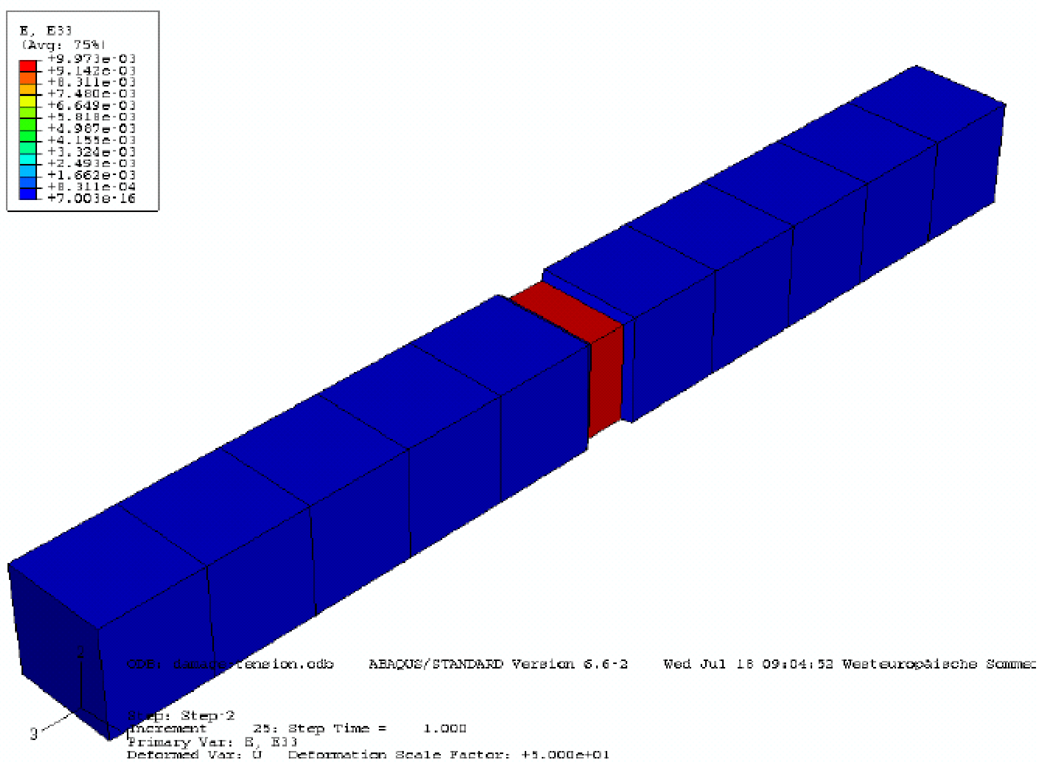

TENSION SOFTENING

Cohesive Interface Elements Eliminate 3-D Cross Effects:

No lateral confinement due to loss of bond.

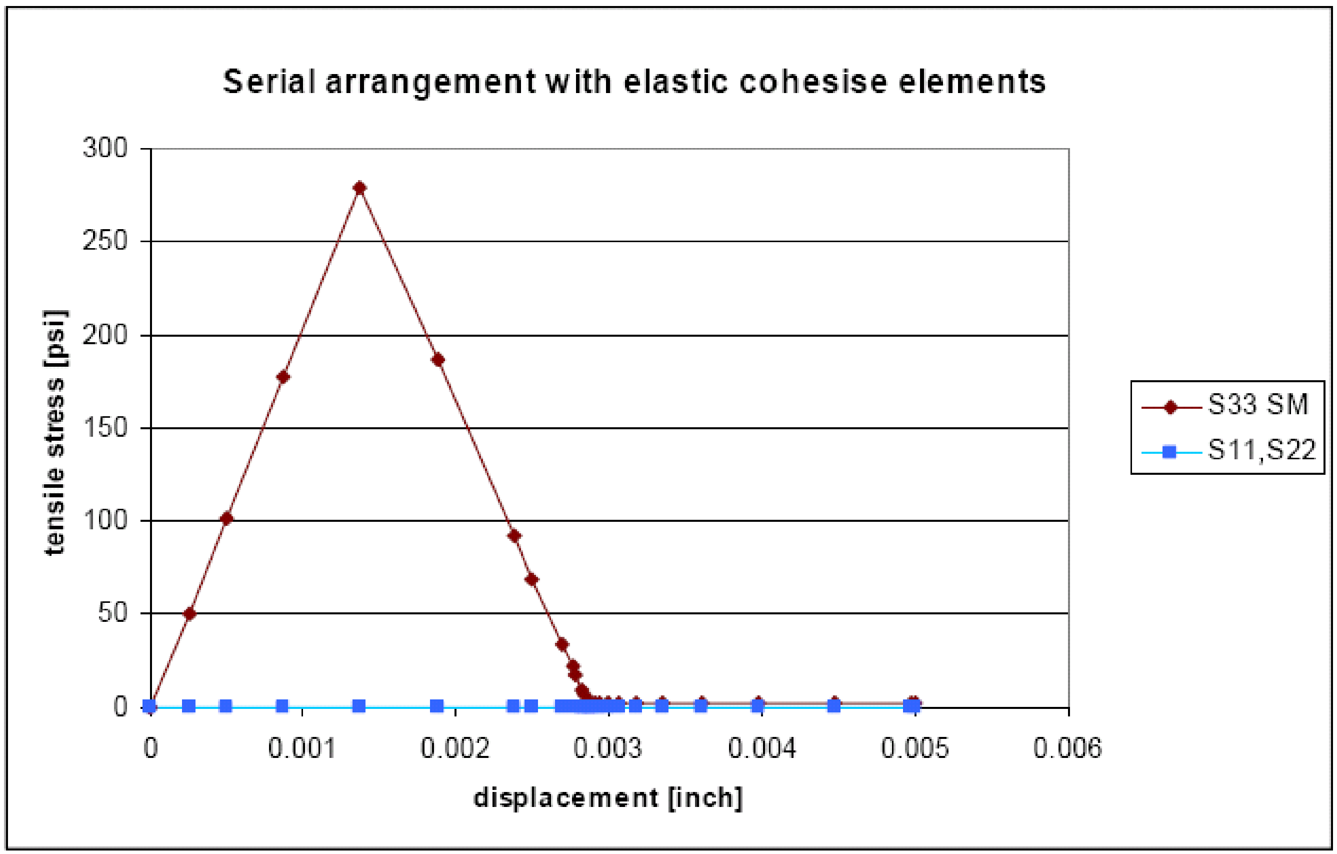

MISMATCH AT PLASTIC SOFTENING-ELASTIC UNLOADING INTERFACE

- Perfect Bond: No Separation-Delamination:
  $u^s_{axial} = u^e_{axial}$ and $u^s_{lat} = u^e_{lat}$ with $\epsilon^s_{lat} = \epsilon^e_{lat}$
- Statics: $\dot{\sigma}^s_{axial} = \dot{\sigma}^e_{axial} = \dot{\sigma}_{axial}$
- Plastic Softening-Elastic Unloading in Axial Tension:
  - Strain Rate in Plastic Softening Domain: $\dot{\boldsymbol{\epsilon}}^s = \boldsymbol{E}_s^{-1}\dot{\boldsymbol{\sigma}} + \dot{\boldsymbol{\epsilon}}_p$
  - Strain Rate in Elastic Unloading Domain: $\dot{\boldsymbol{\epsilon}}^e = \boldsymbol{E}_e^{-1}\dot{\boldsymbol{\sigma}}$
  - Parabolic Drucker-Prager Yield Condition: $F = J_2 + \alpha I_1 - \beta = 0$
    where $\alpha = \frac{1}{3}[f_c - f_t]$ and $\beta = \frac{1}{3} f_c f_t$
  - Associated Plastic Flow Rule: $\dot{\boldsymbol{\epsilon}}_p = \dot{\lambda}\boldsymbol{m} = \dot{\lambda}[\boldsymbol{s} + \alpha\mathbf{1}]$
  - Lateral Plastic Strain Rate: $\dot{\epsilon}_{lat} = \dot{\lambda} m_{lat} = \dot{\lambda}[\frac{1}{3}(\sigma^s_{lat} - \sigma_{axial}) + \alpha]$
- Elastic-Plastic Mismatch due Axial Tension:
  Introduces lateral contraction in softening domain:

$$\dot{\sigma}^s_{lat} = \frac{\nu^s E^e - \nu^e E^s}{E^e(1-\nu^s) + \frac{L^s}{L^e}E^s(1-\nu^e)}\dot{\sigma}_{axial} - \dot{\lambda}E^e[\frac{1}{3}(\sigma^s_{lat} - \sigma_{axial}) + \alpha]$$

BIMATERIAL INTERFACE CONDITIONS

Perfect Bond:

$$[|\mathbf{u}_N|] = \mathbf{u}_N^e - \mathbf{u}_N^s = \mathbf{0} \quad \text{and} \quad [|\mathbf{t}_N|] = \mathbf{t}_N^e - \mathbf{t}_N^s = \mathbf{0}$$

Weak Discontinuities: all strain components exhibit jumps across interface except for $\epsilon_{TT}^e = \epsilon_{TT}^s$ restraint.

Note: Jump of tangential normal stress, $\sigma_{TT}^e \neq \sigma_{TT}^s$.

Imperfect Contact:

$$[|\mathbf{u}_N|] = \mathbf{u}_N^e - \mathbf{u}_N^s \neq \mathbf{0} \quad \text{whereas} \quad [|\mathbf{t}_N|] = \mathbf{t}_N^e - \mathbf{t}_N^s = \mathbf{0}$$

Strong Discontinuities: all displacement components exhibit jumps across interface.

Note: FE Displacement method enforces traction continuity in ‘weak’ sense only, hence $[|\mathbf{t}_N|] \neq 0$.

COMPRESSION SOFTENING

Issue of Material vs Structural Response:

Axial Force Member: compression response of weak element

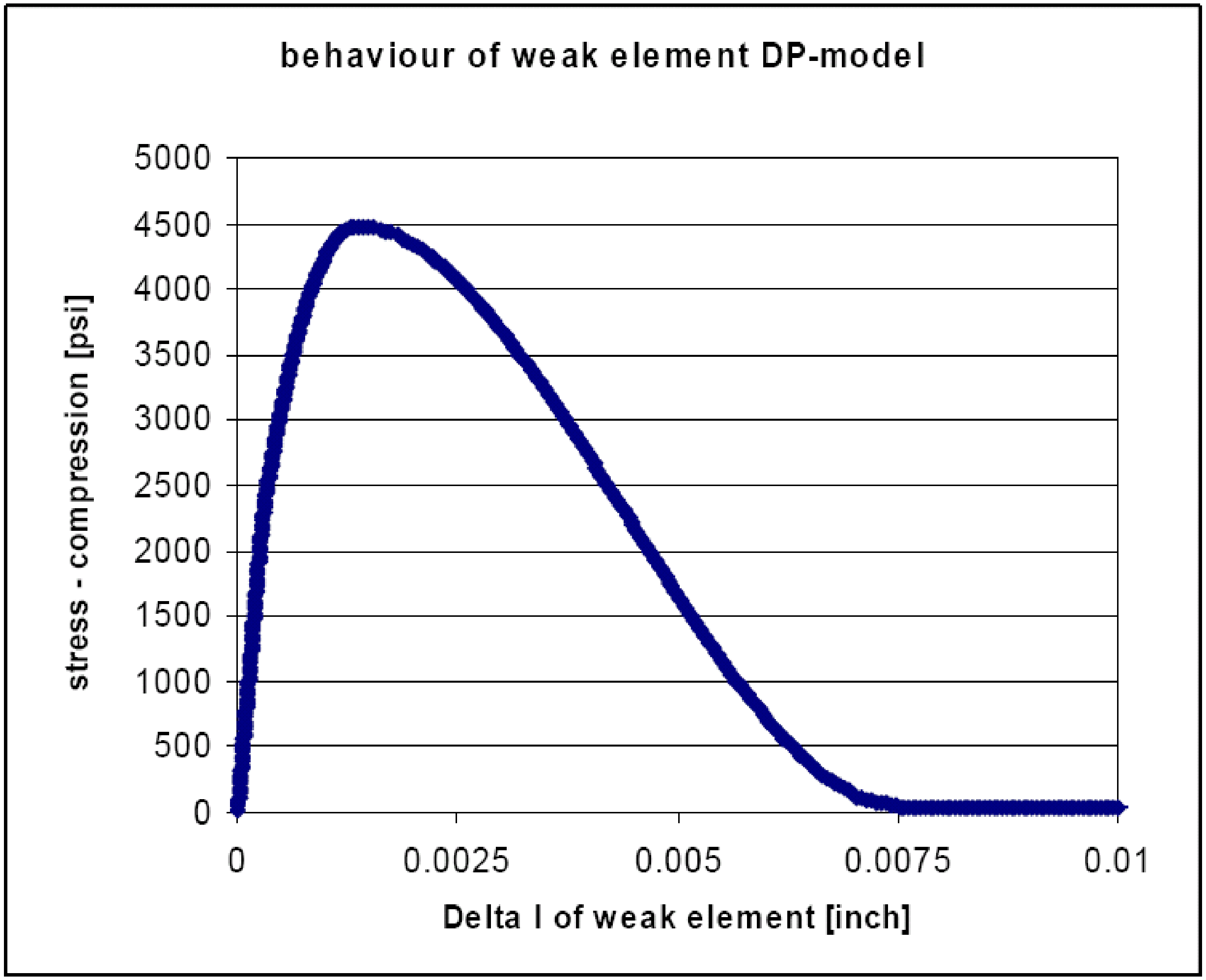

COMPRESSION SOFTENING

Full 3-D Cross Effect:

Lateral confinement introduces uniform triaxial state of stress (elastic if no cap)

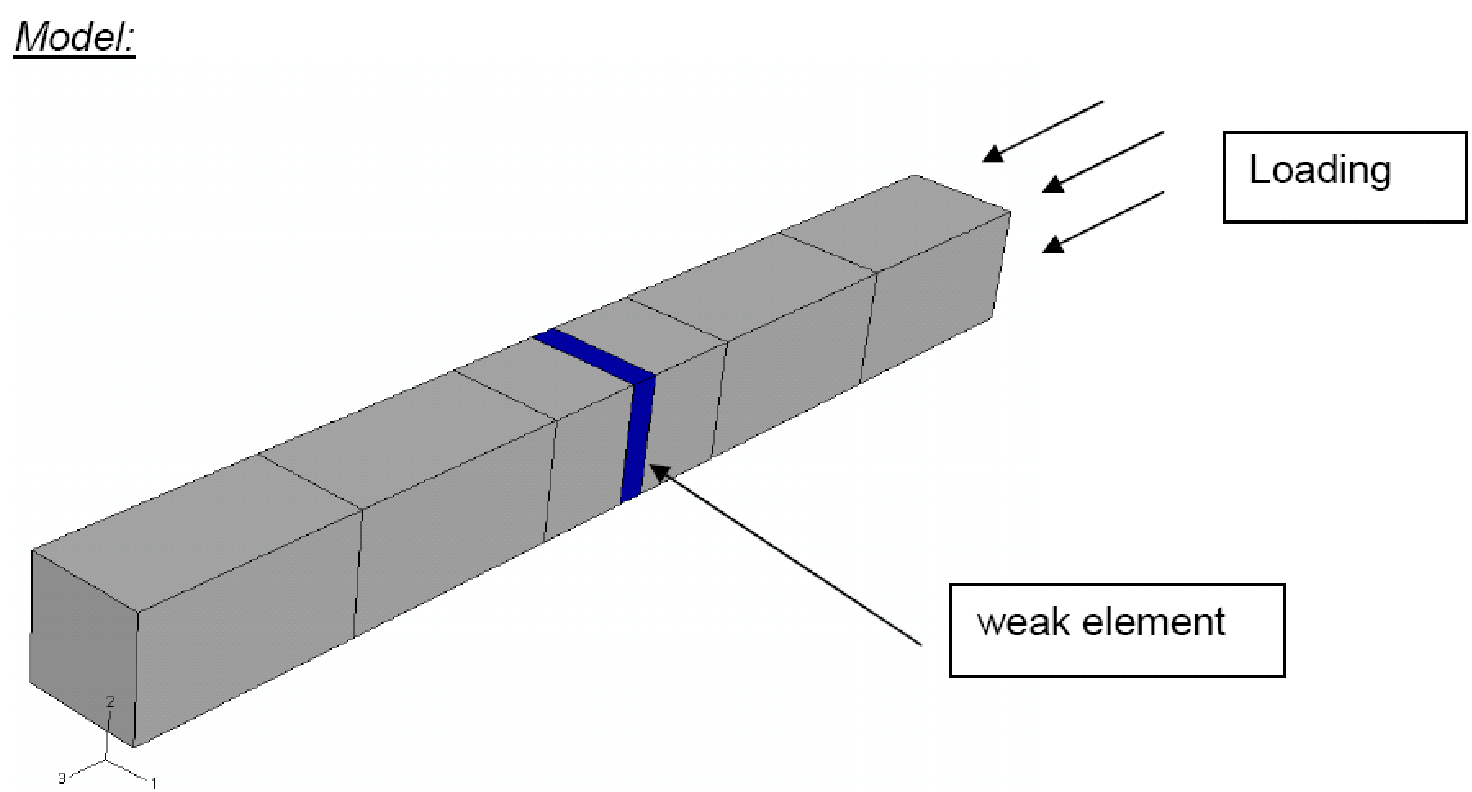

COMPRESSION SOFTENING

3-D Cross Effect: Confinement Introduces Elastic Triaxial Compression

No softening of Damage-Plasticity Model in Abaqus because of missing cap.

Deformed mesh: S33 (magnitude 50)

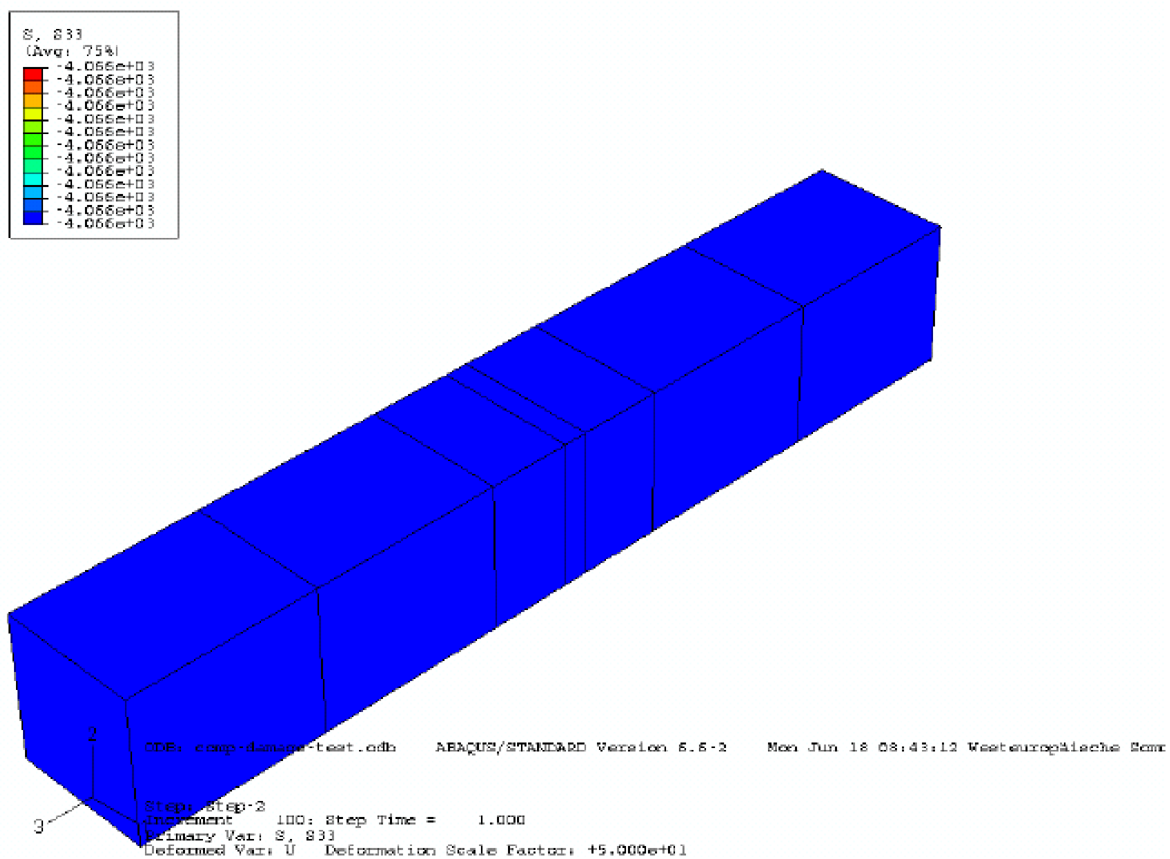

COMPRESSION SOFTENING

Reduction of 3-D Cross Effect:

Cohesive Interface Elements: eliminate lateral confinement

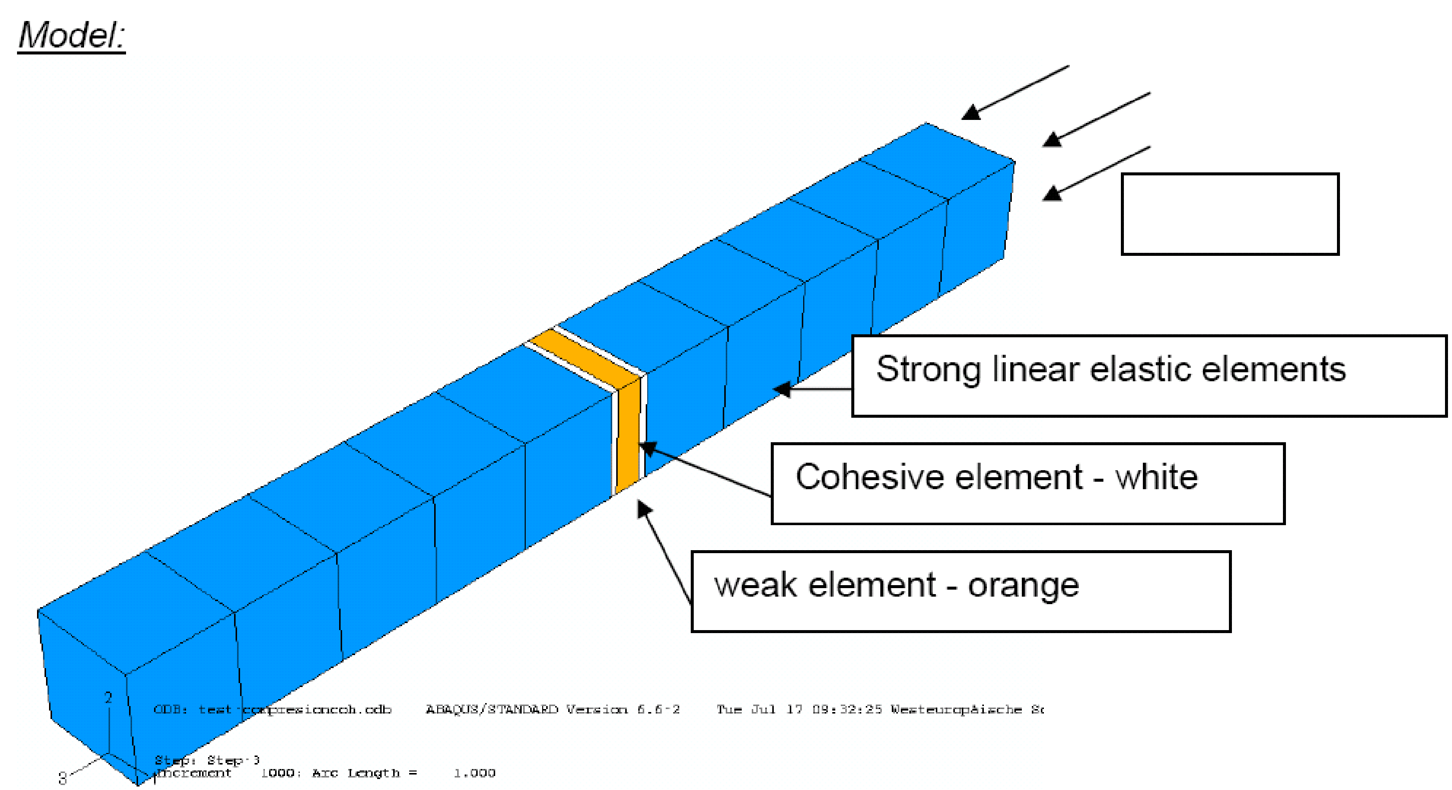

COMPRESSION SOFTENING

Cohesive Interface Elements Eliminate 3-D Cross Effects

Localization of compression failure in weak element.

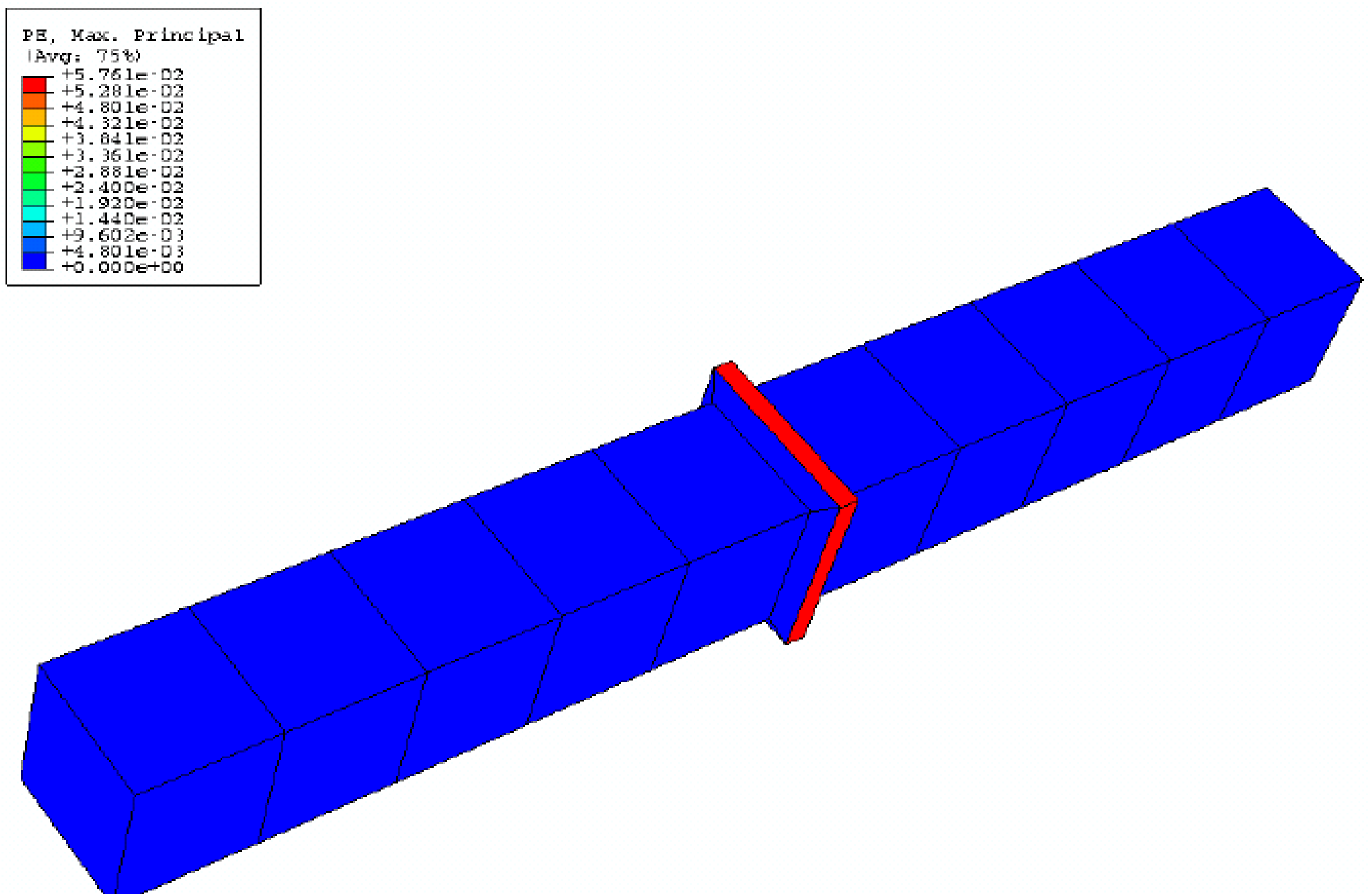

COMPRESSION SOFTENING

Snap-Back due Localization of Compression Failure in Weak Element

Cohesive Interface elements eliminate lateral confinement.

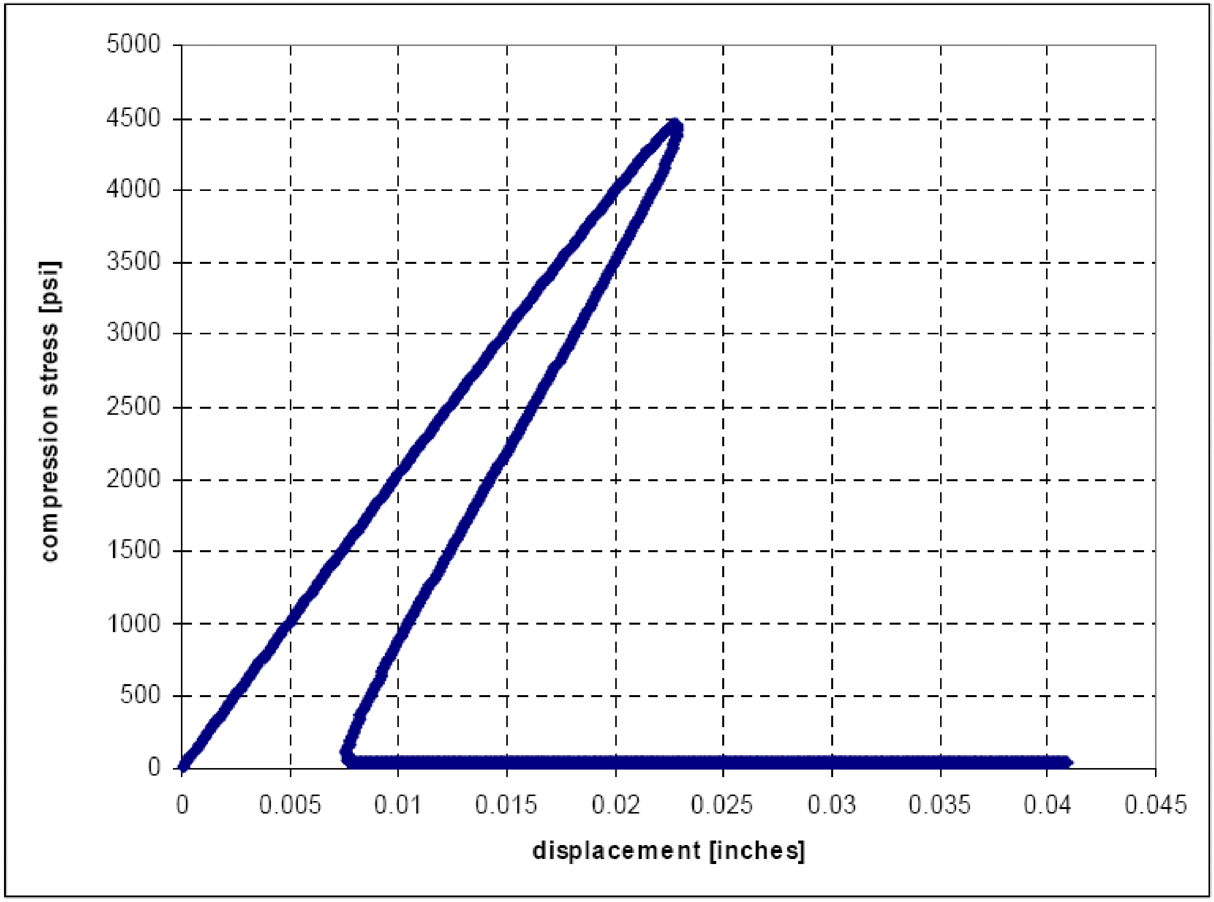

TENSION STIFFENING

Stress Transfer of Parallel System: Full Bond

Kinking iff embedded rebar has no shear and bending stiffness

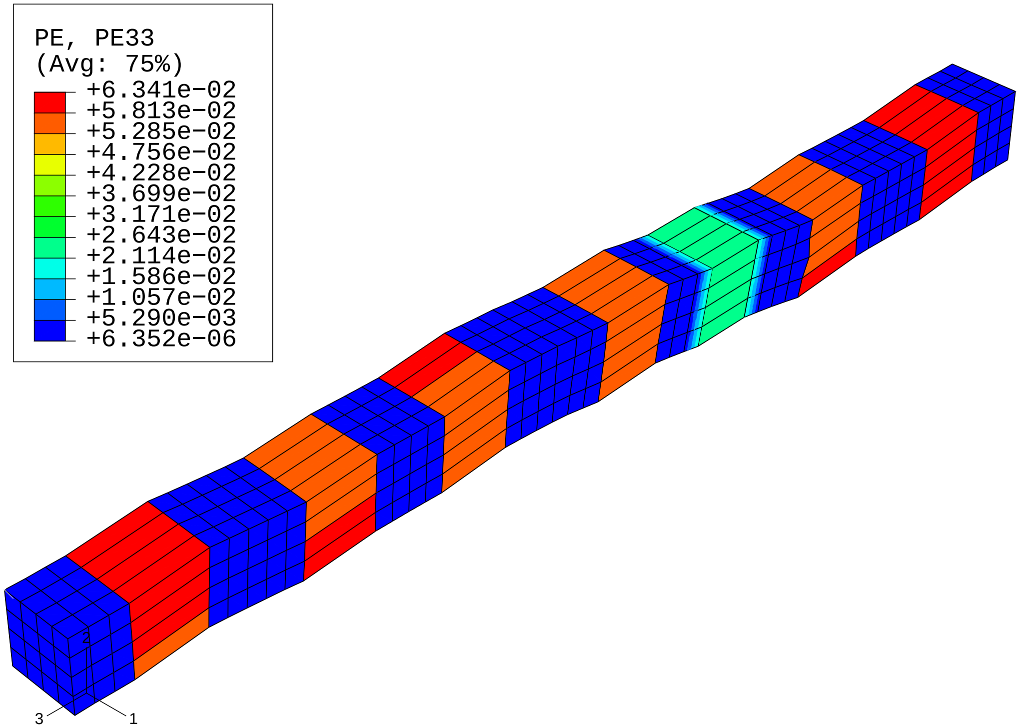

TENSION STIFFENING

Stress Transfer of Parallel System: Full Bond

Mesh Effect for Constant Fracture Energy: $G_f = const.$

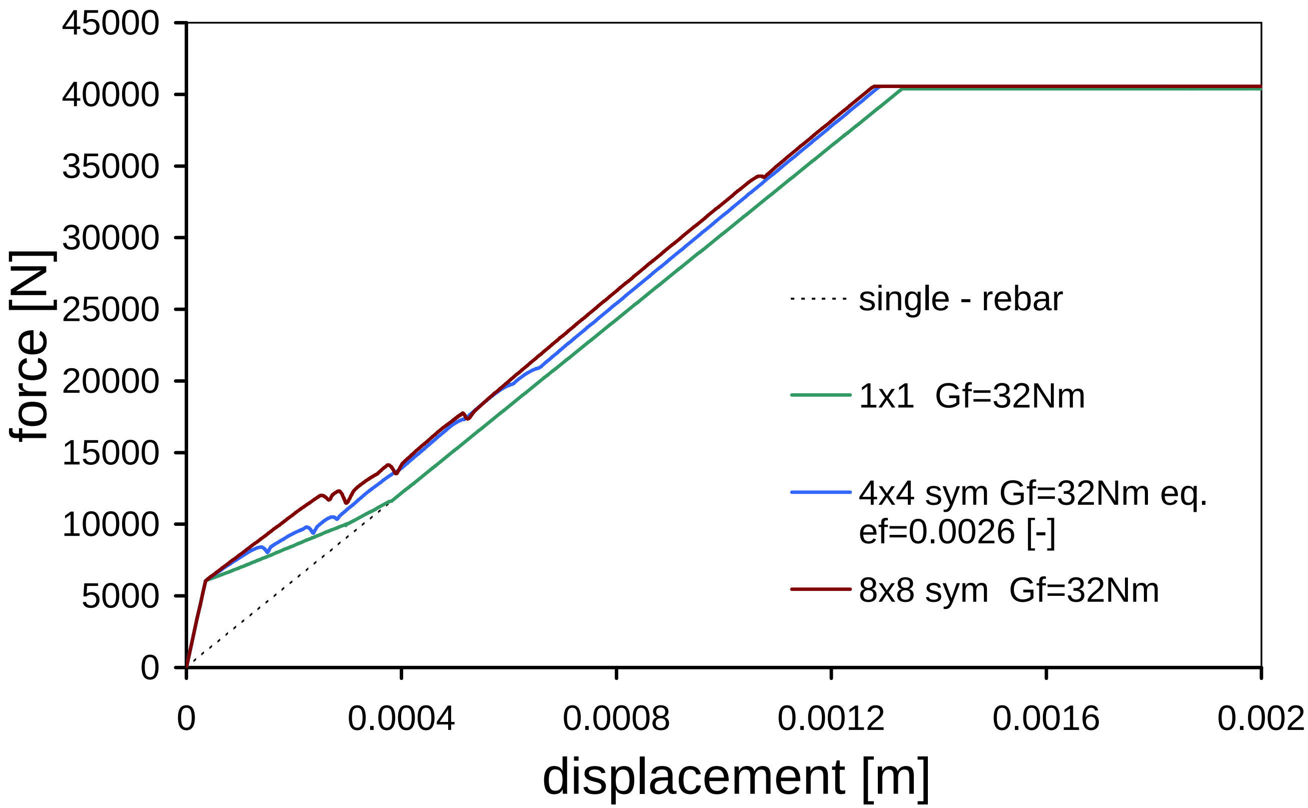

Stress Transfer of Parallel System: Full Bond

Mesh Effect for Constant Cracking Strain: $\epsilon_f = const.$

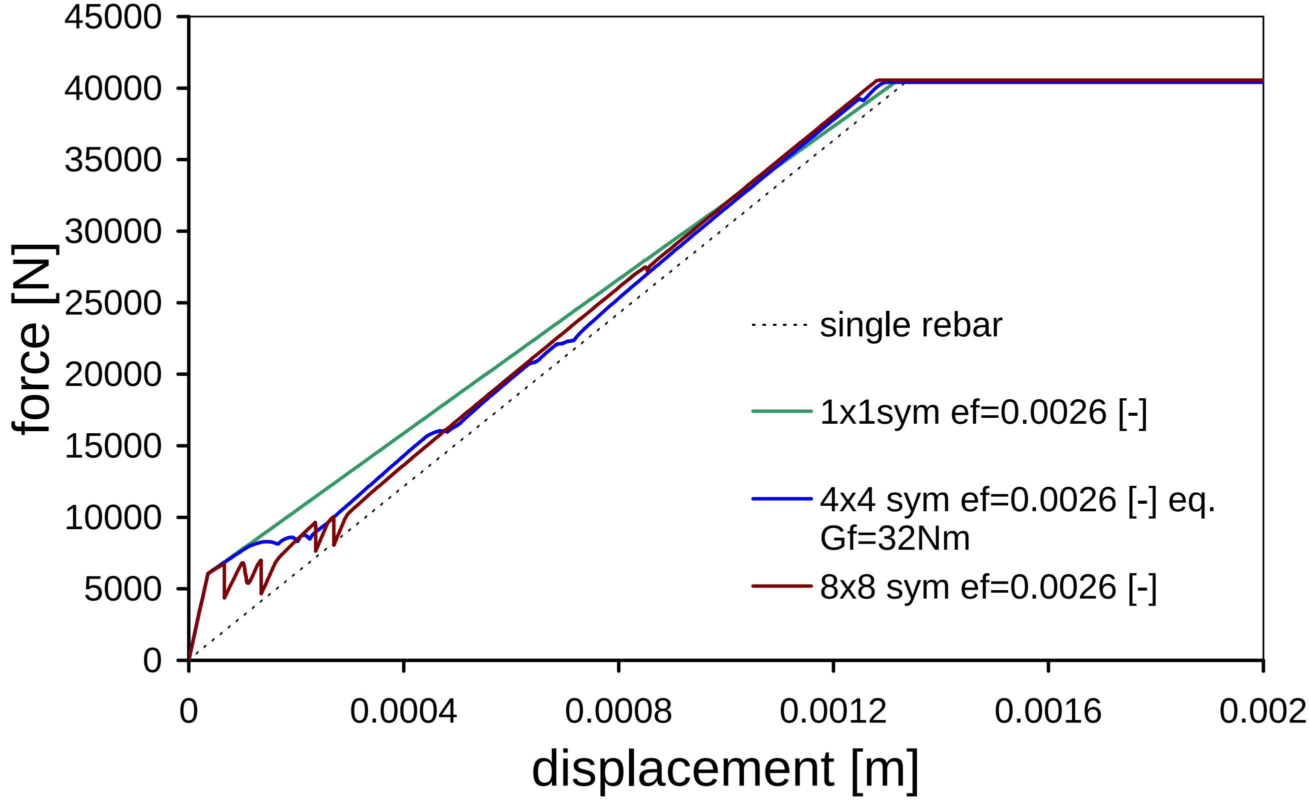

TENSION STIFFENING

Stress Transfer of Parallel System: Full Bond

Regular crack spacing ‘independent’ of mesh size.

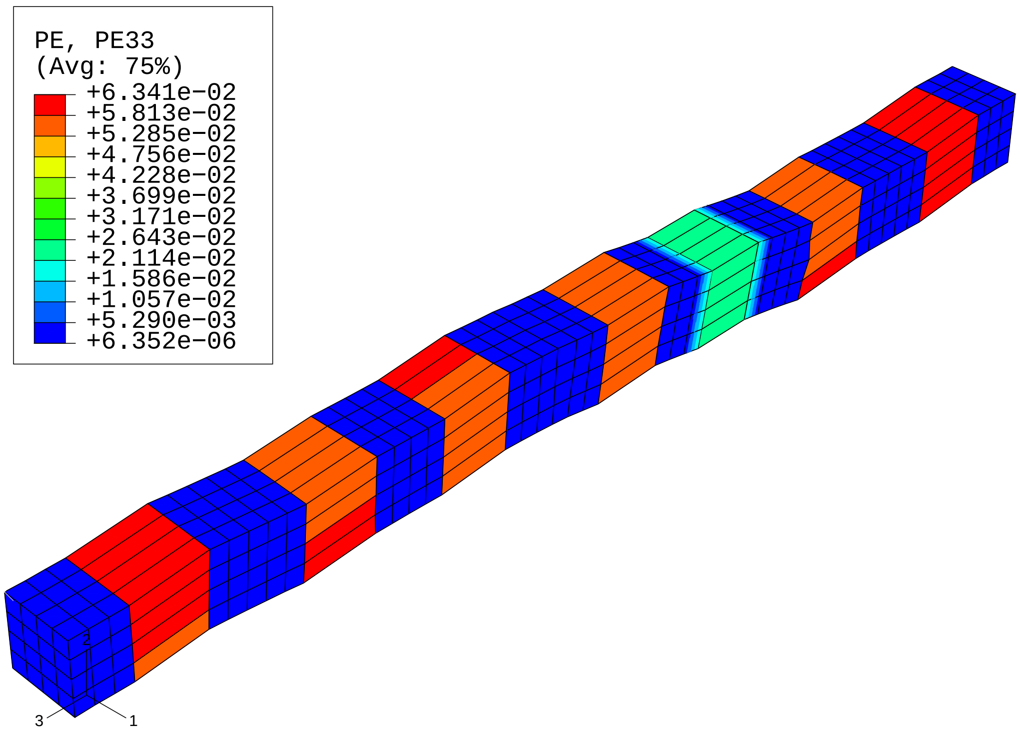

TENSION STIFFENING

Local Study of Stress Transfer in Segment between Adjacent Cracks:

Effect of fracture energy mode II for modeling shear debonding.

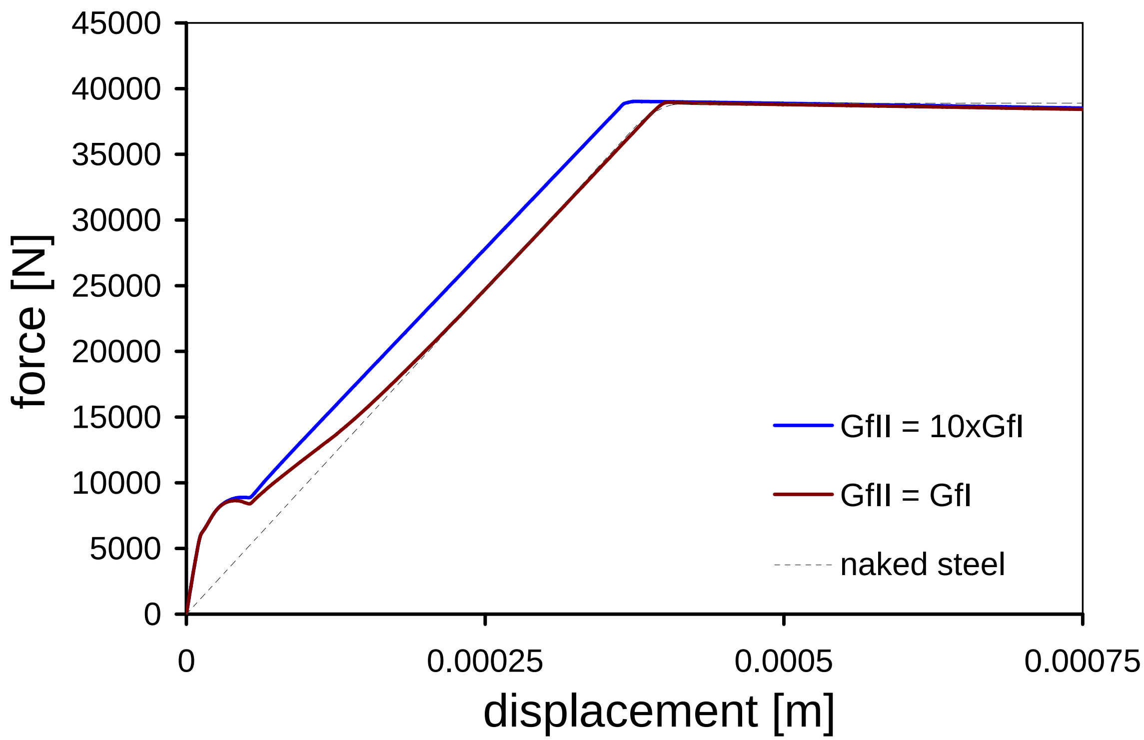

TENSION STIFFENING

Stress Transfer of Parallel System near Center Crack

Shear transfer in steel rebar (von Mises)

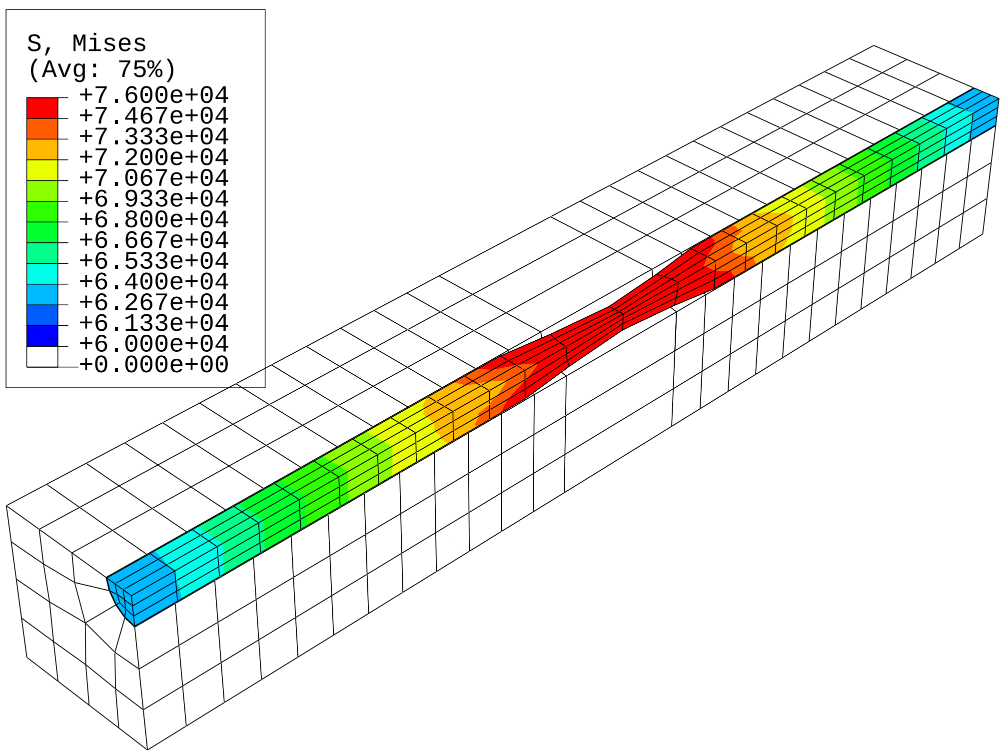

TENSION STIFFENING

Stress Transfer of Parallel System near Center Crack

Shear transfer in concrete (von Mises stress)

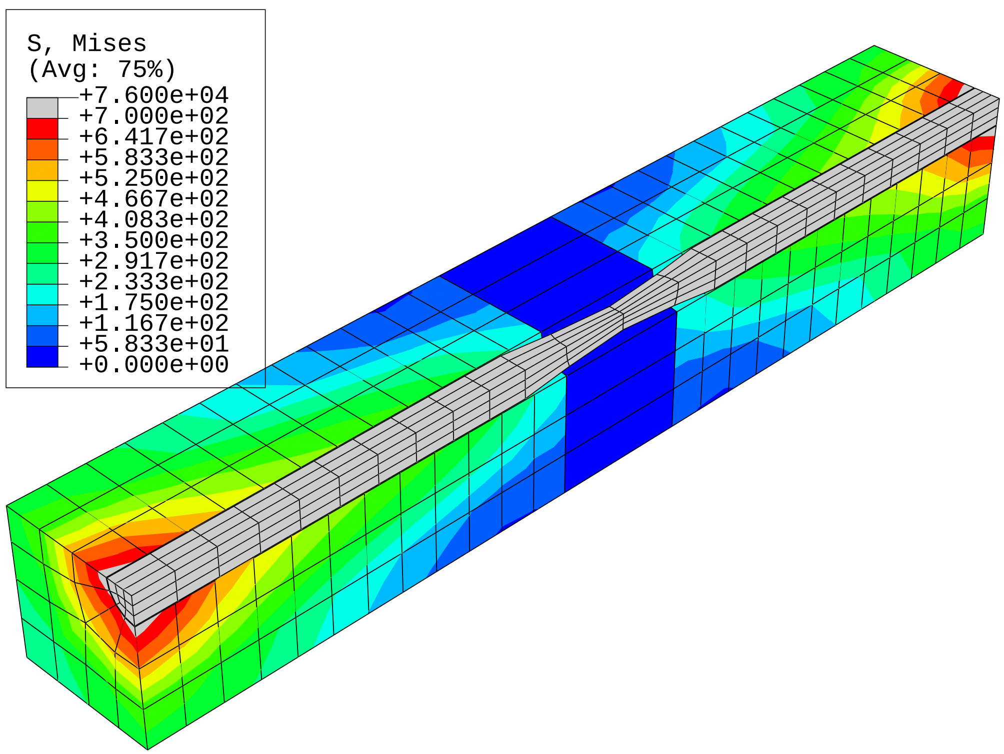

TENSION STIFFENING

Stress Transfer of Parallel System near Center Crack

Axial stress transfer at steel-concrete interface

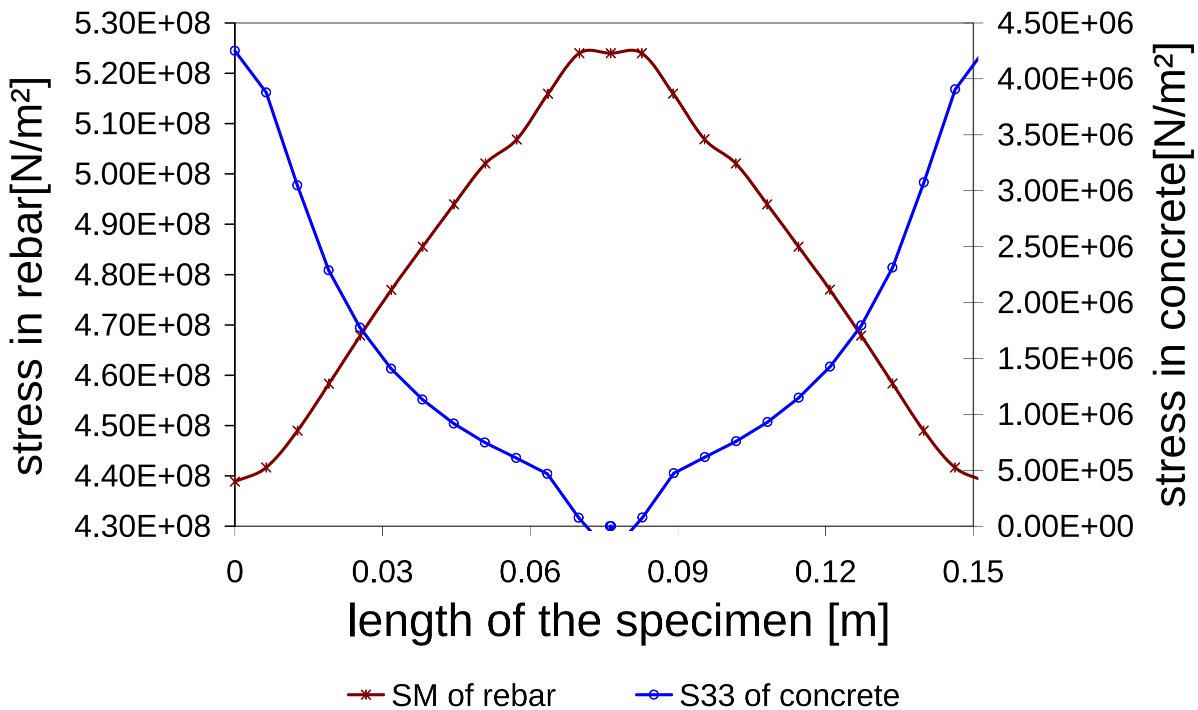

CONCLUDING REMARKS

Main Lessons from Class # 6:

Tension Softening vs Tension Stiffening:

Both Serial and Parallel Systems Exhibit Snap-Back Conditions.

Loss of Bond at Weak Element Interface:

Loss of Triaxial Confinement-No Cross Effects

Loss of Bond at Steel-Concrete Interface:

Tensile Cracking Followed by Shear Debonding